Plant, Cell & Environment

Plant, Cell and Environment (2013) **36**, 721–732 doi: 10.1111/pce.12009

Alternative oxidase impacts the plant response to biotic stress by influencing the mitochondrial generation of reactive oxygen species

MARINA CVETKOVSKA & GREG C. VANLERBERGHE

Departments of Biological Sciences and Cell and Systems Biology, University of Toronto Scarborough, 1265 Military Trail, Toronto, Ontario, Canada M1C 1A4

ABSTRACT

Previously, we showed that inoculation of tobacco with *Pseudomonas syringae* incompatible pv. *maculicola* results in a rapid and persistent burst of superoxide (O_2^-) from mitochondria, no change in amount of mitochondrial alternative oxidase (AOX) and induction of the hypersensitive response (HR). However, inoculation with incompatible pv. *phaseolicola* resulted in increased AOX, no O_2^- burst and no HR. Here, we show that in transgenic plants unable to induce AOX in response to pv. *phaseolicola*, there is now a strong mitochondrial O_2^- burst, similar to that normally seen only with pv. *maculicola*. This interaction did not however result in a HR. This indicates that AOX amount is a key determinant of the mitochondrial O_2^- burst but also that the burst itself is not sufficient to induce the HR. Surprisingly, the O_2^- burst normally seen towards pv. *maculicola* is delayed in plants lacking AOX. This delay is associated with a delayed HR, suggesting that the burst does promote the HR. A O_2^- burst can also be induced by the complex III inhibitor antimycin A (AA), but is again delayed in plants lacking AOX. The similar mitochondrial response induced by pv. *maculicola* and AA suggests that electron transport is a target during HR-inducing biotic interactions.

Key-words: *Nicotiana tabacum*; antimycin A; complex III; hypersensitive response; manganese superoxide dismutase; mitochondrial superoxide burst; nitric oxide; peroxynitrite; programmed cell death; *Pseudomonas syringae*.

Abbreviations: AA, antimycin A; AOX, alternative oxidase; CuZnSOD, copper zinc superoxide dismutase; ETC, electron transport chain; FeSOD, iron superoxide dismutase; HR, hypersensitive response; MnSOD, manganese superoxide dismutase; NO, nitric oxide; O_2^-, superoxide; $ONOO^-$, peroxynitrite; RNS, reactive nitrogen species; ROS, reactive oxygen species; SA, salicylic acid; SOD, superoxide dismutase; WT, wild-type.

Correspondence: G. C. Vanlerberghe. E-mail: gregv@utsc.utoronto.ca

INTRODUCTION

Mitochondrial electron transport chains (ETCs) are a known source of reactive oxygen species (ROS) such as superoxide (O_2^-) and H_2O_2 (Møller 2001; Murphy 2009; Hamanaka & Chandel 2010). Single electron leak from reduced ETC components to oxygen produces O_2^-, and complexes I and III are proposed to be major sites of such electron leak. In the mitochondrial matrix, ETC-generated O_2^- can be converted enzymatically to H_2O_2 by manganese superoxide dismutase (MnSOD). The rate of such ROS generation is strongly dependent upon membrane potential and the reduction state of ETC components, which is turn, is dependent upon the activity of the energy-dissipating systems, particularly oxidative phosphorylation. Hence, when adenosine diphosphate (ADP) is being actively phosphorylated, membrane potential and ROS generation are lower than when ADP is limiting (Møller 2001). More recently, mitochondria have also been recognized as a potential source of nitric oxide (NO) due to single electron leak from ETC components to nitrite. Complex III, cyt c and complex IV have each been postulated as potential sites of such activity (Modolo *et al*. 2005; Planchet *et al*. 2005; Poyton, Ball & Castello 2009; Gupta *et al*. 2011). It is also known that O_2^- and NO can react rapidly to generate peroxynitrite ($ONOO^-$), which has been shown to accumulate in tissues generating ROS and reactive nitrogen species (RNS; Chaki *et al*. 2009, 2011; Gaupels *et al*. 2011; Vandelle & Delledonne 2011; Serrano *et al*. 2012).

Interestingly, the plant mitochondrial ETC includes an alternative oxidase (AOX) that branches from the main respiratory chain, directly coupling the oxidation of ubiquinol with reduction of oxygen to water (Finnegan, Soole & Umbach 2004). AOX is not proton pumping and electron flow to AOX bypasses proton-pumping complexes III and IV. As a result, AOX activity could potentially reduce O_2^- and NO generation, by both moderating membrane potential if ADP is limiting, and by simply reducing electron flow through parts of the respiratory chain that generate these ROS and RNS. Recently, we provided evidence that this is indeed a role for the plant AOX as transgenic plants lacking this branch in the respiratory chain displayed constitutive higher levels of

mitochondria-localized O_2^- and cellular NO (Cvetkovska & Vanlerberghe 2012a).

Plant responses to biotic stress are known to involve dynamic changes in ROS and RNS, which may act as signaling molecules to coordinate plant defence responses, including the hypersensitive response (HR; Torres, Jones & Dangl 2006; Leitner *et al*. 2009; Torres 2010; Vellosillo *et al*. 2010; Coll, Epple & Dangl 2011; Spoel & Loake 2011). Recently, the mitochondrion has emerged as one of the potentially important sources of ROS and RNS during biotic stress responses (Modolo *et al*. 2005; Yao & Greenberg 2006; Amirsadeghi, Robson & Vanlerberghe 2007; Garmier *et al*. 2007; Gleason *et al*. 2011). In this case, AOX may be well positioned to coordinate mitochondrial ROS and RNS signalling. Interestingly, there have been numerous reports regarding the dynamic nature of AOX amount and activity in response to bacterial, viral and fungal pathogens (Lacomme & Roby 1999; Simons *et al*. 1999; Ordog, Higgins & Vanlerberghe 2002; Gilliland *et al*. 2003; Vidal *et al*. 2007; Király *et al*. 2008; Cheng *et al*. 2011; Lee *et al*. 2011). However, a general model for the role and importance of AOX in different biotic stress responses is yet to fully emerge from these studies.

We recently characterized defence responses of *Nicotiana tabacum* to different compatible and incompatible pathovars of the bacterial pathogen *P. syringae* (Cvetkovska & Vanlerberghe 2012b). The incompatible pv. *phaseolicola* elicited well-known defence responses, such as increased salicylic acid (SA) and *PR-1* transcript, but did not elicit HR cell death. On the other hand, the incompatible pv. *maculicola* elicited strong defence responses (such as rapid accumulation of SA, NO and H_2O_2, and induction of HR-associated genes) and the HR. Using fluorescent confocal microscopy and a mitochondrial-localized O_2^- indicator, we showed that the HR, but not the response to pv. *phaseolicola* or to a compatible pathovar, was preceded by an early and persistent burst of O_2^- from mitochondria. By examining changes in AOX and MnSOD, we proposed that the mitochondrial O_2^- burst was supported by a coordinated response of these components. In particular, while pv. *phaseolicola* induced a strong increase in AOX, this was not the case with the HR-inducing pv. *maculicola*. Further, pv *maculicola* induced a specific loss of MnSOD activity over time that was not seen in response to pv. *phaseolicola*. Combined, these changes should support a greater accumulation of mitochondrial O_2^- in response to pv. *maculicola*. In the current work, we have used transgenic plants to test the model that AOX is indeed an important determinant of the mitochondrial O_2^- burst following pathogen infection, as well as to evaluate the significance of this O_2^- burst in the determination of cell fate.

MATERIALS AND METHODS

Plant material and growth conditions

Tobacco (*N. tabacum* L. cv Petit Havana SR1) was used for all experiments. Transgenic lines with suppressed amounts of AOX protein (lines RI9, RI29) as a result of the presence of an *Aox1a* RNA interference construct, or elevated amounts of AOX protein (line B7) as a result of the presence of an *Aox1a* transgene driven by a constitutive promoter, have been previously characterized (Amirsadeghi *et al*. 2006; Wang *et al*. 2011). Plants were grown in controlled-environment chambers (Model PGR-15, Conviron, Winnipeg, MB, Canada) with a 16 h photoperiod, temperature of 28 °C/22 °C (light/dark), relative humidity of 60%, photosynthetic photon flux density of 130 μmol m^{-2} s^{-1}, and in a general purpose growing medium (Pro-mix BX, Premier Horticulture, Rivière-du-Loup, Quebec, Canada). Plants were irrigated with water daily and fertilized with 10x diluted Hoagland's solution three times per week. Plants were used 5–6 weeks after initiating germination in vermiculite.

Bacteria and plant inoculations

Pseudomonas syringae pv. *maculicola* ES4326 and pv. *phaseolicola* NP3121 were each acquired from Dr. K. Yoshioka, University of Toronto. Bacteria were cultured in King's B medium (King, Ward & Raney 1954), either without antibiotic (pv. *maculicola*), or with 50 μg mL^{-1} rifampicin (pv. *phaseolicola*). Bacteria were grown overnight with rotation (28 °C, ~20 rpm), washed once and resuspended in distilled water. Culture density was determined by absorbance at 600 nm using a spectrophotometer (HP8452, Agilent Technologies, Mississauga, Canada). Unless stated otherwise, density was adjusted to 1×10^7 cfu mL^{-1} for plant inoculations, care being taken to inoculate comparable leaves between plants. Plants were inoculated at 5 h into the light period by completely infiltrating with liquid the abaxial side of the second to lowest true leaf, using a syringe with needle. Mock-inoculated plants were infiltrated with distilled water. Bacterial growth *in planta* and ion leakage of leaf tissue were each determined as previously described (Cvetkovska & Vanlerberghe 2012b).

Imaging of leaf mitochondrial O_2^- and leaf NO and $ONOO^-$

Imaging of ROS and RNS was performed using confocal fluorescent microscopy, similar to previously described (Cvetkovska & Vanlerberghe 2012a). Briefly, imaging of O_2^- was performed using the MitoSOX Red mitochondrial O_2^- indicator (M36008; Invitrogen, Carlsbad, CA, USA) that is selectively accumulated by mitochondria, where it is oxidized by O_2^- and becomes fluorescent upon binding nucleic acid (Robinson, Janes & Beckman 2008). Leaf NO was detected using DAF-FM diacetate NO indicator (D23844; Invitrogen), which after crossing the plasma membrane is cleaved by esterases to generate intracellular DAF-FM, which is then oxidized specifically by NO to produce a fluorescent product (Kojima *et al*. 1999). Leaf $ONOO^-$ was detected using APF (A36003; Invitrogen) that becomes

fluorescent after reacting with $ONOO^-$ (Setsukinai *et al.* 2003). In some cases, leaf was also labelled with Mitotracker Red (M7512; Invitrogen) that selectively accumulates in mitochondria.

At different times, following inoculation with bacteria or mock inoculation with H_2O, tobacco leaves were removed and the lower epidermis was peeled off. The remaining leaf segments were then floated (30 min, RT, dark) on either 3 μM MitoSOX Red (in water), 10 μM DAF-FM diacetate (in water), or 10 μM APF (in 10 mM KH_2PO_4, pH 7.4). In some cases, leaf segments were double-labelled by also including 0.35 μM MitoTracker Red in the floating solution. Samples were then mounted on microscope slides and the mesophyll cell layer immediately examined with a LSM510 META laser-scanning confocal microscope (Carl Zeiss, Jena, Germany) with appropriate excitation/detection settings (MitoSOX Red, 488/585–615 nm; MitoTracker Red, 543/585–615 nm; DAF-FM diacetate, 488/500–530 nm; APF, 488/500–530 nm).

All images were acquired under similar acquisition settings. Z-series, typically 8–16 μm in depth with 2 μm step size, were combined in a maximum intensity projection image using LSM510 imaging software. Co-localization, after double-labelling experiments, was analysed after thresholding for image background noise using JACoP, a plug-in for the software Image J (Bolte & Cordelieres 2006). In our analysis, the Manders' coefficient represents the fraction of pixels from the red fluorescence channel that overlap with the green fluorescence channel. All images were analysed as Z-series to ensure that the areas of co-localization existed in all three dimensions.

For antimycin A (AA) experiments, tobacco leaves were removed and the lower epidermis peeled off. The remaining leaf segments were then floated (RT, dark) on water or 10 μM AA (A-8674; Sigma-Aldrich). After the floating treatments (1 h or 4 h), leaves were processed for confocal microscopy imaging, as described above.

Other analyses

Leaf superoxide dismutase (SOD) activities [MnSOD, copper zinc SOD (CuZnSOD), iron SOD (FeSOD)] were determined using an activity gel assay, as previously described (Cvetkovska & Vanlerberghe 2012b). H_2O_2 amount in tobacco leaf was determined using a biochemical assay, as previously described (Cvetkovska & Vanlerberghe 2012b).

RESULTS

Plant responses to different incompatible pathovars of *P. syringae*

When infiltrated with the incompatible bacterial pathogen *P. syringae* pv. *maculicola*, leaves of tobacco display a resistance response that includes the HR (Cvetkovska & Vanlerberghe 2012b). To study the impact of AOX on this resistance response, we compared the HR of wild-type (WT) tobacco to that of two transgenic lines (RI9, RI29) with silenced AOX expression. As expected, measures of leaf conductivity indicated a substantial loss of membrane integrity (a measure of HR cell death) in the WT by 1 d post-inoculation, with some further loss of membrane integrity up to 3 d post-inoculation (Fig. 1a). However, the two transgenic lines lacking AOX displayed a significant delay in HR cell death in response to pv. *maculicola* (Fig. 1a). These plants showed little change in conductivity by 1 d post-inoculation, particularly the RI9 plants. In plants lacking AOX, it took until 3 d post-inoculation (RI29) or 4 d post-inoculation (RI9) before conductivity reached a level similar to that since in the WT by 1 d (Fig. 1a). The dramatic difference in kinetics of cell death between the WT and transgenic lines was not the result of differences in the rate of bacterial proliferation. In WT and transgenic lines, there was a similar and dramatic proliferation of the bacteria by 1 d post-inoculation and some further modest proliferation by 2 d (Fig. 1c).

When infiltrated with the incompatible *P. syringae* pv. *phaseolicola*, leaves of tobacco display a resistance response but this response does not include the HR, and hence, no significant loss of membrane integrity is observed (Fig. 1b; Cvetkovska & Vanlerberghe 2012b). Similarly, transgenic lines lacking AOX showed no change in membrane integrity following inoculation with pv. *phaseolicola* (Fig. 1b). In WT and transgenic lines, there was a similar and only very modest increase in bacterial numbers in the leaf following inoculation with pv. *phaseolicola* (Fig. 1d).

Previously, we showed that inoculation with pv. *maculicola* is associated with a rapid and persistent burst of O_2^- from mitochondria, while no such burst is seen in response to pv. *phaseolicola*. We hypothesized that this may have been due to differences in AOX level, which remains low after inoculation with pv. *maculicola* but increases rapidly in response to pv. *phaseolicola* (Cvetkovska & Vanlerberghe 2012b). To test this model, we used confocal microscopy to image mitochondrial O_2^- after a mock inoculation with water or inoculation with bacteria. (Note that Supporting Information Fig. S1 is a typical example of the mesophyll cell images found throughout this manuscript. Supporting Information Figure S1 compares the bright-field, chlorophyll autofluorescence, fluorescence (MitoSOX) and merged images, and is meant to aid interpretation of the images found throughout this manuscript). Similar to our previous findings (Cvetkovska & Vanlerberghe 2012a) we found that transgenic plants lacking AOX have higher levels of mitochondrial O_2^- than WT plants under control (in this case mock-inoculated) leaves (Fig. 2). As expected, inoculation of WT tobacco with pv. *phaseolicola* did not result in any elevation of mitochondrial O_2^- (i.e. no O_2^- burst; Fig. 2). However, in transgenic plants unable to induce AOX in response to inoculation with pv. *phaseolicola*, we now observed an early and persistent increase in mitochondrial O_2^- in response to this pathovar, despite these plants already having higher control (mock-inoculated) levels of mitochondrial O_2^- than WT (Fig. 2).

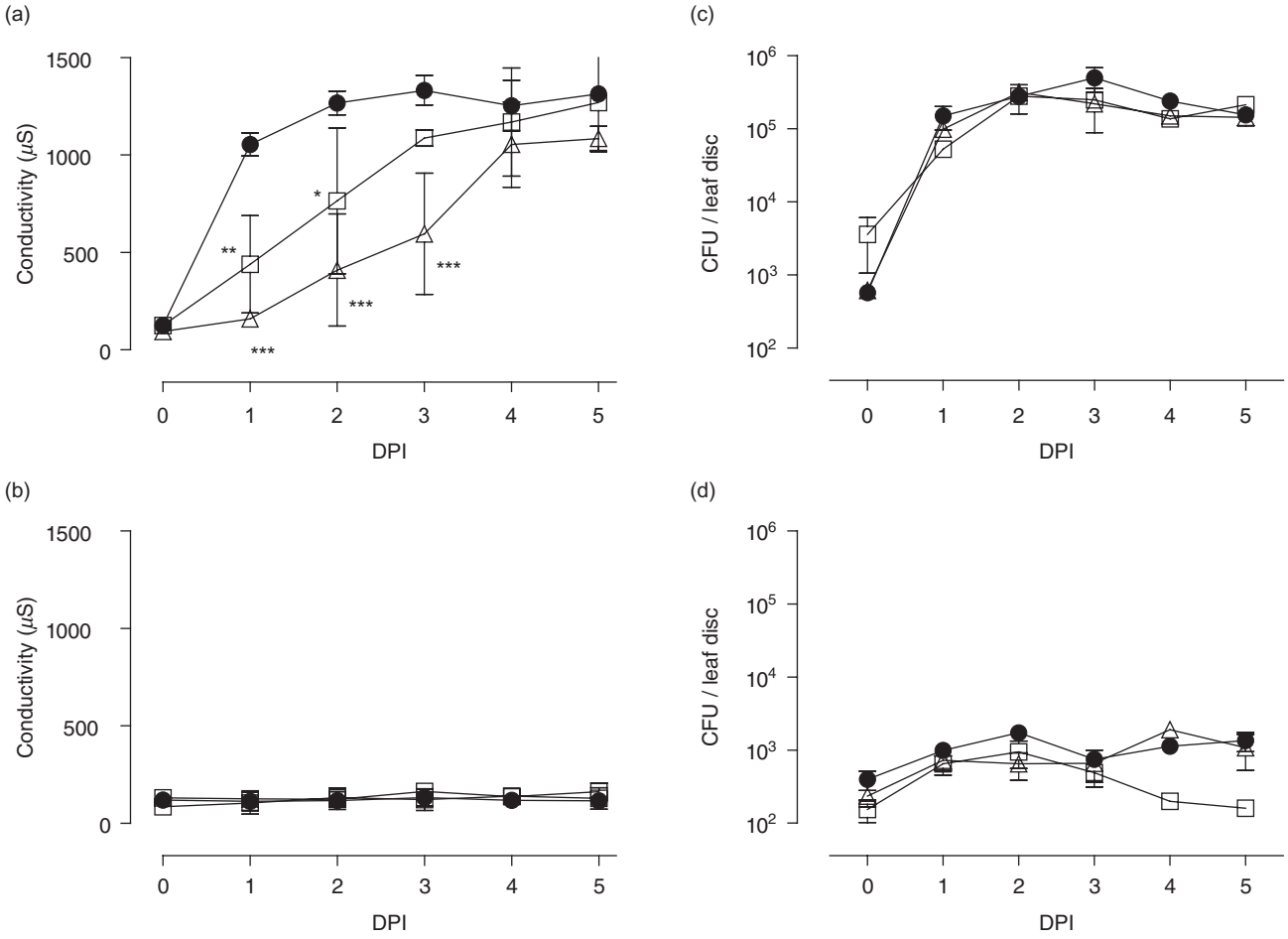

Figure 1. Conductivity (ion leakage) of tobacco leaf (a,b) and bacterial proliferation in tobacco leaf (c,d) at different times post-inoculation with *P. syringae* pv. *maculicola* (a,c) or pv. *phaseolicola* (b,d). Tobacco lines tested included the WT (closed circle) and two transgenic lines with suppressed levels of AOX (RI9, open triangle; RI29, open square). For bacterial proliferation experiments, bacterial density for inoculation was adjusted to 1×10^5 cfu mL^{-1}. Data are the mean ± SE of three independent experiments (conductivity) or two independent experiments (proliferation). Data were analysed by two-way ANOVA followed by a Bonferroni post-test to compare at each time point the WT line to each transgenic line. Number of asterisks indicates the level of significant difference: $*P < 0.05$; $**P < 0.01$; $***P < 0.001$. Data points without an asterisk are not significantly different from the WT.

As expected, inoculation of WT tobacco with pv. *maculicola* resulted in a strong mitochondrial O_2^- burst that was readily evident at 4 h post-inoculation and persisted through 24 h (Fig. 3). Surprisingly, this O_2^- burst was noticeably delayed in transgenic plants lacking AOX. In this case, there was little evidence of the O_2^- burst at 4 h (i.e. levels were similar to the mock-inoculated transgenic plants). However, by 24 h, the burst was apparent and of similar intensity to the WT (Fig. 3).

We examined whether the delay in the O_2^- burst in transgenic plants lacking AOX in response to pv. *maculicola* was perhaps due to higher steady-state levels of MnSOD or other SOD isozyme activity in the transgenic plants. However, SOD activity gels did not indicate any significant differences between WT and transgenic plants, either before or after inoculation with bacteria (Fig. 4). In particular, MnSOD activity was similar between WT and transgenic plants before inoculation and this activity declined similarly in each plant line in response to pv. *maculicola* (Fig. 4a). This decline was similar to that previously reported (Cvetkovska & Vanlerberghe 2012b). The decline did appear slightly exaggerated in the transgenic lines (particularly at 24 h) but this was not statistically significant and would not, regardless, explain the delayed burst of O_2^- in these lines. There was also no significant difference in SOD activities between WT and transgenic lines in response to pv. *phaseolicola* (Supporting Information Fig. S2).

Given some of the differences seen in mitochondrial O_2^-, we also examined levels of H_2O_2. In this case, a biochemical assay was used to establish whole-leaf levels of this ROS species. As reported previously (Cvetkovska & Vanlerberghe 2012a), transgenic plants lacking AOX actually tended to have lower levels of H_2O_2 than WT in control (time 0, uninoculated) leaves (Fig. 5). Despite this difference in initial H_2O_2 level, the WT and transgenic plants responded similarly to inoculation with pv. *maculicola*. The

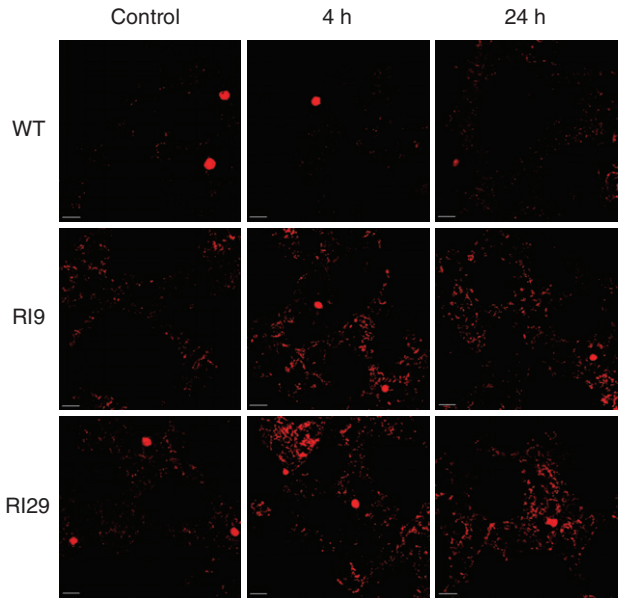

Figure 2. Laser-scanning confocal microscope images of mitochondrial O_2^- in tobacco mesophyll cells at different times post-inoculation with *P. syringae* pv. *phaseolicola*. Tobacco lines tested include the WT and two transgenic lines with suppressed levels of AOX (RI9, RI29). All images are maximum intensity projections of Z-series (8–16 μm in depth) and are representative results from three independent experiments, each of which showed similar results. The control plants (mock-inoculated with H_2O) were similar at 4 h and 24 h, so only images taken at 24 h are shown here. Scale bar = 20 μm.

response was reminiscent of a classical two-phase oxidative burst, with an early rise at 2 h post-inoculation, followed by a decline, and then a second rise at 8 h post-inoculation (Fig. 5a). Nonetheless, these data were quite variable. A fundamental difference between the WT and transgenic lines was seen in response to pv. *phaseolicola*. The WT simply displayed a modest decline in H_2O_2 after inoculation, as reported before (Fig. 5b; Cvetkovska & Vanlerberghe 2012b). However, the transgenic lines displayed an early and greater than twofold *increase* in H_2O_2 that then persisted through 24 h. Despite this fundamental difference in the response of H_2O_2, the *absolute* level of H_2O_2 was not statistically different between the WT and transgenic lines after inoculation, owing it seems to the differences in the initial level (time 0, uninoculated) of this ROS species between WT and transgenic plants.

We next examined the two RNS, NO and $ONOO^-$ that have also been implicated to have a role in biotic stress responses and to perhaps originate (at least in part) from mitochondria (see Introduction). As reported previously (Cvetkovska & Vanlerberghe 2012a), we found that transgenic plants lacking AOX have higher cellular levels of NO than WT plants under control (in this case mock-inoculated) leaves (Fig. 6, Supporting Information Fig. S3). As reported, NO level was particularly enhanced in RI29 (the stronger knockdown) while the amount of NO in RI9 was only modestly higher than in the WT. There was little change in NO amount in any of the plant lines in response to pv. *phaseolicola* (Supporting Information Fig. S3). In response to pv. *maculicola*, NO level in the WT increased dramatically by 4 h post-inoculation, and this level persisted through 24 h (Fig. 6). A similar pattern was evident in RI9 and RI29 except that RI29 consistently displayed less NO than the WT at 24 h post-inoculation.

The amount of $ONOO^-$ was low in mock-inoculated WT and transgenic lines (Fig. 7, Supporting Information Fig. S4). Similar to NO and O_2^-, there was little change in $ONOO^-$ in WT leaves after inoculation with pv. *phaseolicola* (Supporting Information Fig. S4). In this case, there was also little difference between the WT and transgenic lines, either before or after inoculation. Inoculation with pv. *maculicola* increased the amount of $ONOO^-$ in both the WT and transgenic lines after 4 h (Fig. 7). By 24 h, $ONOO^-$ levels were still high, but in this case were also noticeably higher in the transgenic lines compared to WT.

Plant responses to the complex III inhibitor AA

Given the surprising result that transgenic plants lacking AOX display a noticeable delay in the mitochondrial O_2^- burst after inoculation with pv. *maculicola* (Fig. 3), we also characterized the response of WT and transgenic lines to the complex III inhibitor AA. At 1 h after inhibition of complex III, WT plants displayed a large mitochondrial O_2^-

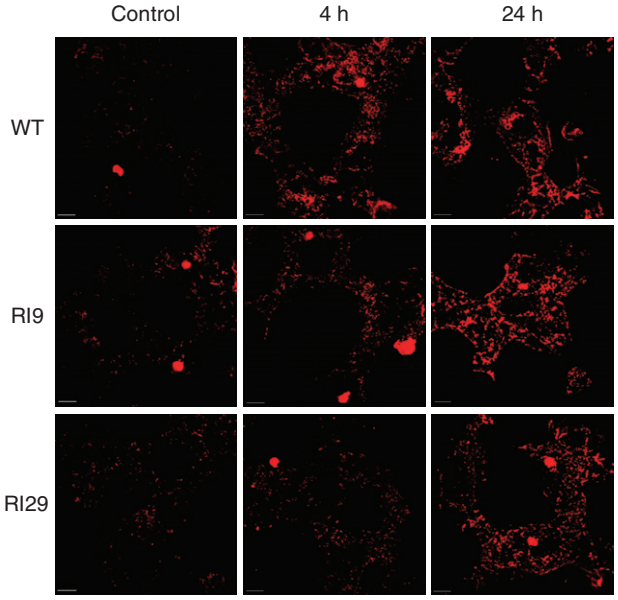

Figure 3. Laser-scanning confocal microscope images of mitochondrial O_2^- in tobacco mesophyll cells at different times post-inoculation with *P. syringae* pv. *maculicola*. Tobacco lines tested include the WT and two transgenic lines with suppressed levels of AOX (RI9, RI29). All images are maximum intensity projections of Z-series (8–16 μm in depth) and are representative results from three independent experiments, each of which showed similar results. The control plants (mock-inoculated with H_2O) were similar at 4 h and 24 h, so only images taken at 24 h are shown here. Scale bar = 20 μm.

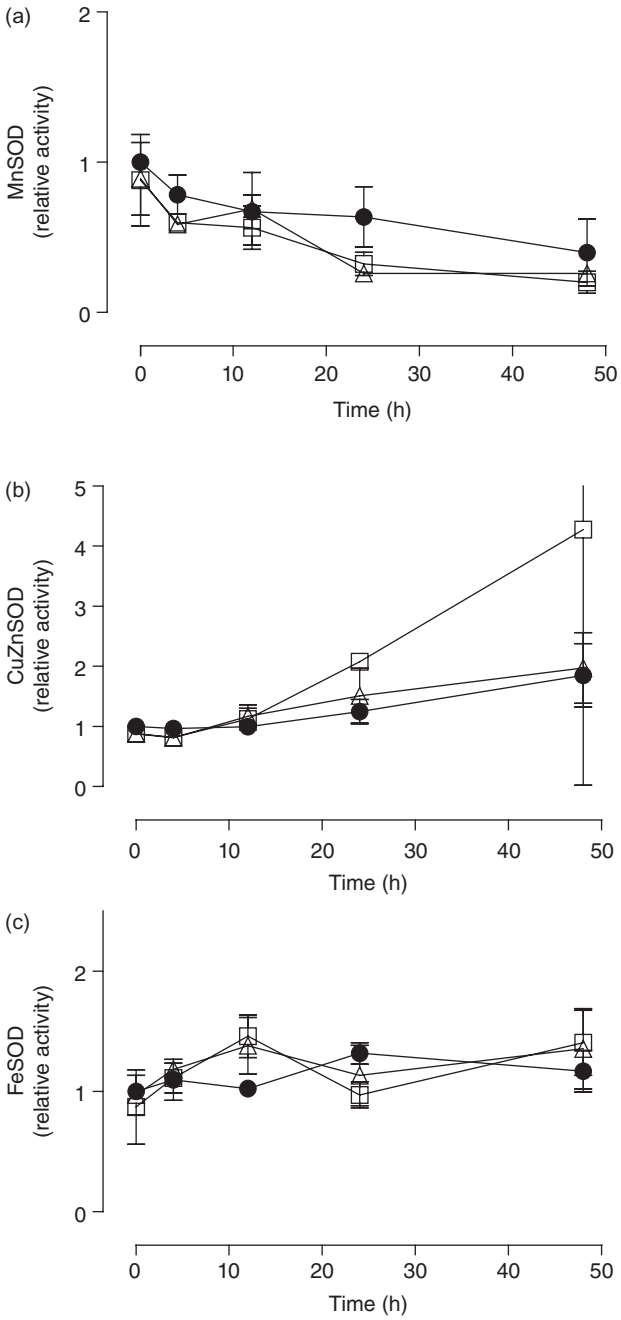

Figure 4. MnSOD (a), CuZnSOD (b) and FeSOD (c) activity in tobacco leaf at different times post-inoculation with *P. syringae* pv. *maculicola*. Tobacco lines tested included the WT (closed circle) and two transgenic lines with suppressed levels of AOX (RI9, open triangle; RI29, open square). Data are the mean ± SE of two independent experiments. Data are relative to the SOD activity of the WT at time 0, which was set to 1.

burst which then largely disappeared by 4 h (Fig. 8). This corresponded with a large increase in *Aox1a* transcript by this time point (data not shown). In plants lacking AOX (RI29), just the opposite pattern was seen. That is, no increase in O_2^- was evident at 1 h after AA, but the burst was very evident at 4 h (i.e. the burst was delayed relative to WT). In contrast, transgenic plants with constitutive over-expression of AOX (line B7) showed no increase in O_2^- at either 1 h or 4 h after AA treatment (Fig. 8).

The amount of NO was also examined in response to AA and the results mirrored those seen with O_2^-. WT plants displayed a large increase in NO at 1 h after AA and this amount decreased by 4 h (Fig. 9). RI29 showed only a modest increase in NO (above its control level) at 1 h, but NO was then very high by 4 h. Finally, B7 plants showed little change in NO level at 1 h and only a small increase at 4 h post-AA treatment.

The amount of $ONOO^-$ was also examined and generally indicative of the O_2^- and NO results described above. In the WT, $ONOO^-$ increased strongly by 1 h after AA treatment and was then similar at 4 h. In RI29, the increase in $ONOO^-$ was only modest at 1 h but then very high at 4 h. In B7, no increase in $ONOO^-$ was evident at 1 h and only a modest increase was seen at 4 h (Fig. 10).

Experiments examining the amount of NO or $ONOO^-$ were done as double-labelling experiments, in which the tissues were also labelled with Mitotracker Red. Analysis of

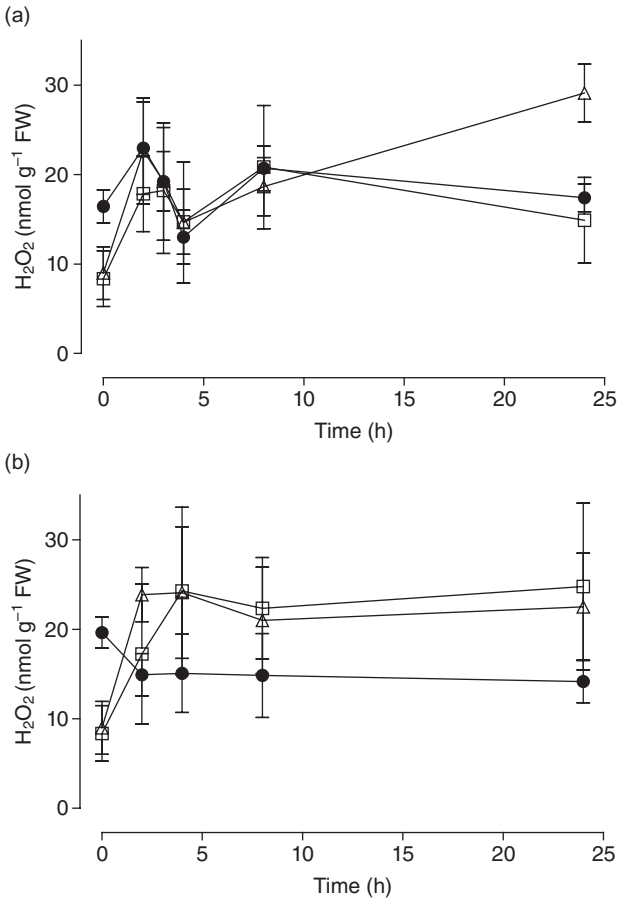

Figure 5. H_2O_2 level in tobacco leaf at different times post-inoculation with *P. syringae* pv. *maculicola* (a) or pv. *phaseolicola* (b). Tobacco lines tested included the WT (closed circle) and two transgenic lines with suppressed levels of AOX (RI9, open triangle; RI29, open square). Data are the mean ± SE of three independent experiments.

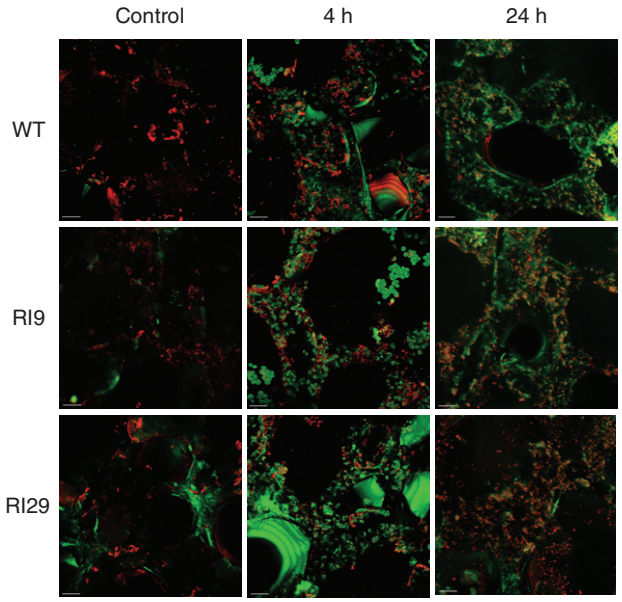

Figure 6. Laser-scanning confocal microscope images of cellular NO in tobacco mesophyll cells at different times post-inoculation with *P. syringae* pv. *maculicola*. Tobacco lines tested include the WT and two transgenic lines with suppressed levels of AOX (RI9, RI29). All images are maximum intensity projections of Z-series (8–16 μm in depth) and are representative results from three independent experiments, each of which showed similar results. All images are double-labelled with DAF-FM and Mitotracker Red to image both NO (green) and mitochondria (red). Co-localization of these signals is yellow. The control plants (mock-inoculated with H_2O) were similar at 4 h and 24 h, so only images taken at 24 h are shown here. Scale bar = 20 μm.

these images indicated a dramatically increased co-localization of mitochondrial signal with NO and $ONOO^-$ signal in the WT by 1 h post-AA treatment, followed by a slight reduction in co-localization by 4 h (Fig. 11). A similar result was seen for RI29, except that the degree of co-localization for both NO and $ONOO^-$ was slightly less at 1 h and slightly greater at 4 h than that seen in the WT. In B7, there was little effect of AA on co-localization of mitochondria with either NO or $ONOO^-$ at 1 h, although some increase was evident by 4 h (Fig. 11).

DISCUSSION

Evidence that the level of AOX is an important determinant of the mitochondrial O_2^- burst

Previously, we showed that inoculation of *N. tabacum* with *P. syringae* pv. *maculicola* was associated with a rapid and persistent burst of O_2^- from mitochondria, no change in the level of AOX, and an induction of the HR. On the other hand, inoculation with pv. *phaseolicola* was associated with a rapid increase in AOX amount, no mitochondrial O_2^- burst and no HR (Cvetkovska & Vanlerberghe 2012b). We hypothesized that AOX level was a critical determinant of the differential response of tobacco to the two bacterial pathovars. Our current results confirm this. In transgenic lines incapable of AOX induction, a O_2^- burst is now generated in response to pv. *phaseolicola*. This is strong evidence that the rapid induction of AOX normally seen in WT tobacco in response to this pathovar is indeed a critical event in preventing the mitochondrial O_2^- burst.

Our results indicate that, in the absence of AOX induction, inoculation with pv. *phaseolicola* does provide all the necessary conditions for a mitochondrial O_2^- burst to occur. However, these same results provide clear evidence that the O_2^- burst is not, in itself, sufficient to generate the HR. While inoculation of plants lacking AOX with pv. *phaseolicola* display an early and persistent O_2^- burst very similar to that of WT plants inoculated with pv. *maculicola*, this does not provoke cell death. This is not surprising and is consistent with hypotheses that the HR is dependent upon multiple coordinating signals that are invoked in response to some incompatible interactions (Mur *et al.* 2008; Coll, Epple & Dangl 2011). For example, despite the similar O_2^- bursts, other ROS and RNS dynamics were clearly different. While inoculation of WT plants with pv. *maculicola* results in a biphasic generation of H_2O_2, this is not the case after inoculation of RI9 and RI29 with pv. *phaseolicola*. Interestingly, while H_2O_2 level tended to decrease in WT plants in response to pv. *phaseolicola*, just the opposite was seen in

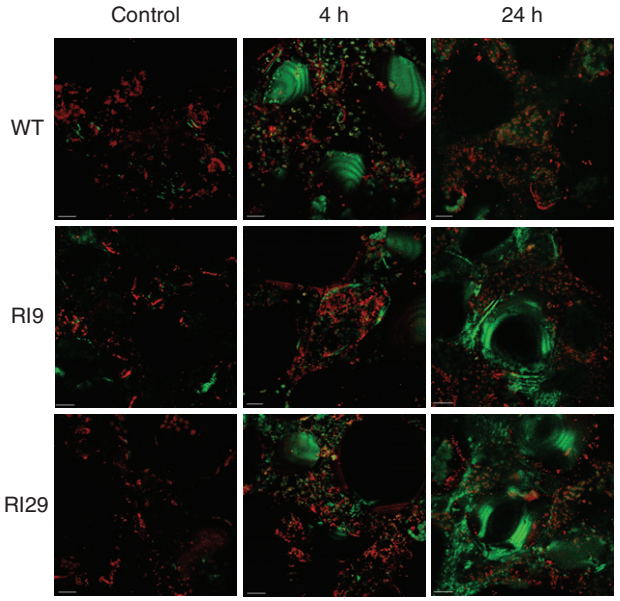

Figure 7. Laser-scanning confocal microscope images of cellular $ONOO^-$ in tobacco mesophyll cells at different times post-inoculation with *P. syringae* pv. *maculicola*. Tobacco lines tested include the WT and two transgenic lines with suppressed levels of AOX (RI9, RI29). All images are maximum intensity projections of Z-series (8–16 μm in depth) and are representative results from three independent experiments, each of which showed similar results. All images are double-labelled with APF and Mitotracker Red to image both $ONOO^-$ (green) and mitochondria (red). Co-localization of these signals is yellow. The control plants (mock-inoculated with H_2O) were similar at 4 h and 24 h, so only images taken at 24 h are shown here. Scale bar = 20 μm.

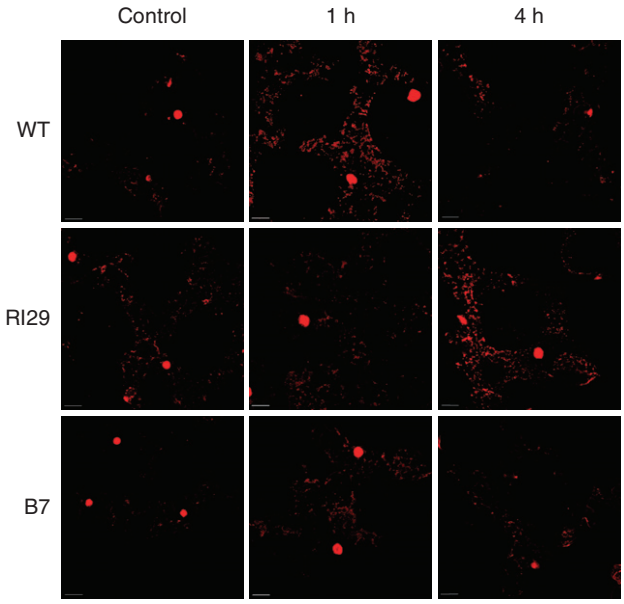

Figure 8. Laser-scanning confocal microscope images of mitochondrial O_2^- in tobacco mesophyll cells at different times following treatment with the complex III inhibitor AA (10 μM). Tobacco lines tested include the WT, a transgenic line with suppressed levels of AOX (RI29) and a transgenic line overexpressing AOX (B7). All images are maximum intensity projections of Z-series (8–16 μm in depth) and are representative results from three independent experiments, each of which showed similar results. The control plants (floated on water without AA) were similar at 1 h and 4 h, so only images taken at 1 h are shown here. Scale bar = 20 μm.

RI9 and RI29. It seems possible that this is due to the O_2^- burst, unique to the transgenic lines, providing substrate for H_2O_2 generation. In addition, while the interaction of WT plants with pv. *maculicola* is associated with a NO burst, we found no evidence of such a burst in RI9 and RI29 plants responding to pv. *phaseolicola*.

Evidence that the mitochondrial O_2^- burst does promote the HR

It is generally accepted that ROS and RNS are important players in the initiation and execution of the HR and other defence responses in plants (see Introduction). However, the relative importance of different ROS and RNS, the importance of timing and localization of their dynamics, and the molecular detail of their roles are not yet well understood. Our results provide evidence that the mitochondrial O_2^- burst does promote the HR to *P. syringae* (although it is not sufficient to induce the HR, as discussed earlier). In particular, we found that transgenic plants lacking AOX display a delay in the O_2^- burst in response to pv. *maculicola*, and this results in a significantly delayed HR. Interestingly, while the O_2^- burst caused by pv. *maculicola* was delayed in these plants, the rise in NO was not. Similarly, we saw no significant differences in H_2O_2 dynamics between lines after inoculation with pv. *maculicola*. Hence, the delayed HR does not appear to be associated with substantial differences in NO or H_2O_2 dynamics but is rather more specifically related to the timing of the O_2^- burst. It suggests that the mitochondrial O_2^- burst enhances the progression of the HR. This adds to other literature indicating that mitochondrial-derived ROS are associated with the HR (Naton, Hahlbrock & Schmelzer 1996; Yao *et al*. 2002; Yao & Greenberg 2006; Garmier *et al*. 2007; Pattanayak *et al*. 2012).

Evidence that the mitochondrion is a target of biotic stress

To further examine the potential role of mitochondria in biotic stress, we examined whether parallels exist between the response to bacterial infection and the response to a well-defined mitochondrial disruption, that being a restriction of electron flow through complex III. It was previously shown that, for tobacco cells under a normal growth condition, the maximal capacity of AOX to support electron flow to O_2 is much less than the steady-state O_2 consumption rate of the cell (Vanlerberghe & McIntosh 1992, 1994). Hence, following inhibition of complex III by AA, there is a sharp decline in O_2 consumption to a rate equivalent to the

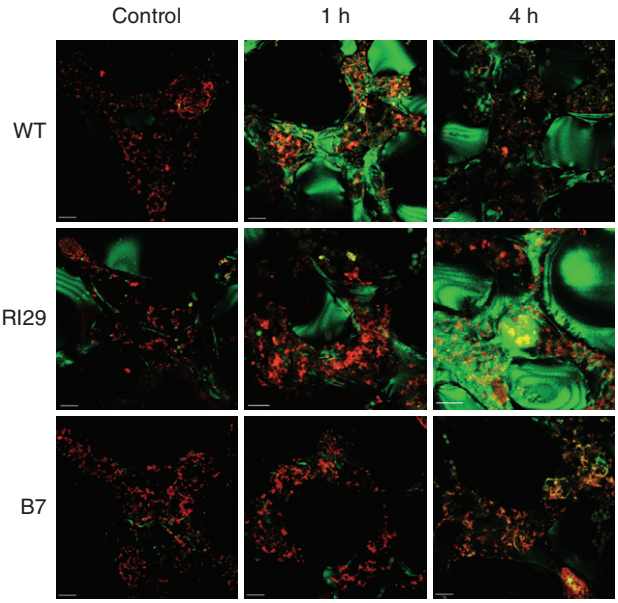

Figure 9. Laser-scanning confocal microscope images of cellular NO in tobacco mesophyll cells at different times following treatment with the complex III inhibitor AA (10 μM). Tobacco lines tested include the WT, a transgenic line with suppressed levels of AOX (RI29) and a transgenic line overexpressing AOX (B7). All images are maximum intensity projections of Z-series (8–16 μm in depth) and are representative results from three independent experiments, each of which showed similar results. All images are double-labelled with DAF-FM and Mitotracker Red to image both NO (green) and mitochondria (red). Co-localization of these signals is yellow. The control plants (floated on water without AA) were similar at 1 h and 4 h, so only images taken at 1 h are shown here. Scale bar = 20 μm.

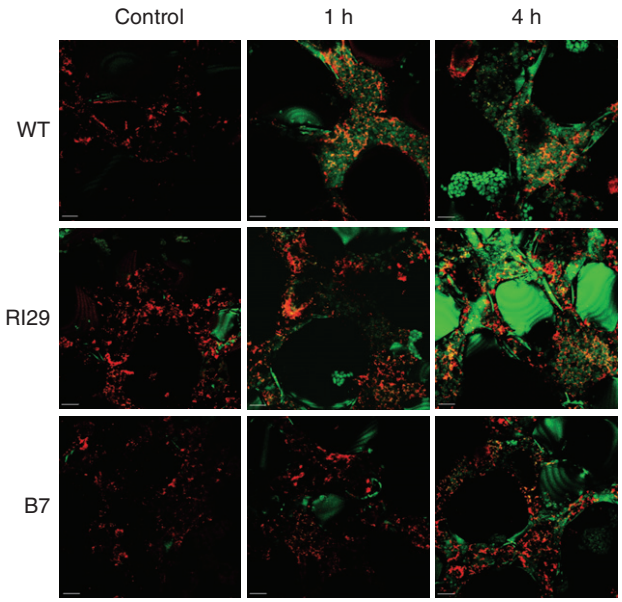

Figure 10. Laser-scanning confocal microscope images of cellular $ONOO^-$ in tobacco mesophyll cells at different times following treatment with the complex III inhibitor AA (10 μM). Tobacco lines tested include the WT, a transgenic line with suppressed levels of AOX (RI29) and a transgenic line overexpressing AOX (B7). All images are maximum intensity projections of Z-series (8–16 μm in depth) and are representative results from three independent experiments, each of which showed similar results. All images are double-labelled with APF and Mitotracker Red to image both $ONOO^-$ (green) and mitochondria (red). Co-localization of these signals is yellow. The control plants (floated on water without AA) were similar at 1 h and 4 h, so only images taken at 1 h are shown here. Scale bar = 20 μm.

maximal capacity of AOX. However, the reduced O_2 consumption rate is transient because the inhibition of the cytochrome pathway results in a strong induction of *Aox1a* mRNA and AOX protein, which is then able to support much greater rates of electron flow to O_2 (Vanlerberghe & McIntosh 1992, 1994).

We found that treatment of WT tobacco leaf with AA resulted in a large increase in both mitochondrial O_2^- and cellular NO. Co-localization analyses confirmed that a significant portion of the NO being detected was localized to mitochondria. These findings are in keeping with the hypothesis that over-reduction of ETC components, such as would occur after inhibition of electron flow by AA, increases the generation of O_2^- and NO by the respiratory chain (Poyton *et al.* 2009; Cvetkovska & Vanlerberghe 2012a). However, the increase in O_2^- and NO was clearly transient, as the high levels observed at 1 h post-AA were largely disappeared by 4 h. Our interpretation is that this is due to the induction of AOX in the longer term, and is supported by the results observed with transgenic plants. B7 plants did not display an increase in O_2^- or NO at either 1 h or 4 h after inhibition of complex III since these plants were able to use the constitutive high level of AOX to maintain electron flow, even shortly after AA treatment.

Plants lacking AOX (RI29) displayed a particularly interesting pattern of O_2^- and NO generation in response to AA. One might expect that the level of O_2^- and NO in these plants at 1 h post-AA should be as high or higher than seen in the WT since these plants completely lack AOX as an electron sink. Instead, these plants displayed a clear delay in both O_2^- and NO generation, in which levels remained low at 1 h (when levels were high in the WT) but then increased dramatically at 4 h, when levels were already declined in the WT. At present, we do not understand the ability of these transgenic plants to avoid (albeit only in the short term) an increased generation of ROS and RNS after inhibition of the cytochrome pathway. In the case of O_2^-, it does not

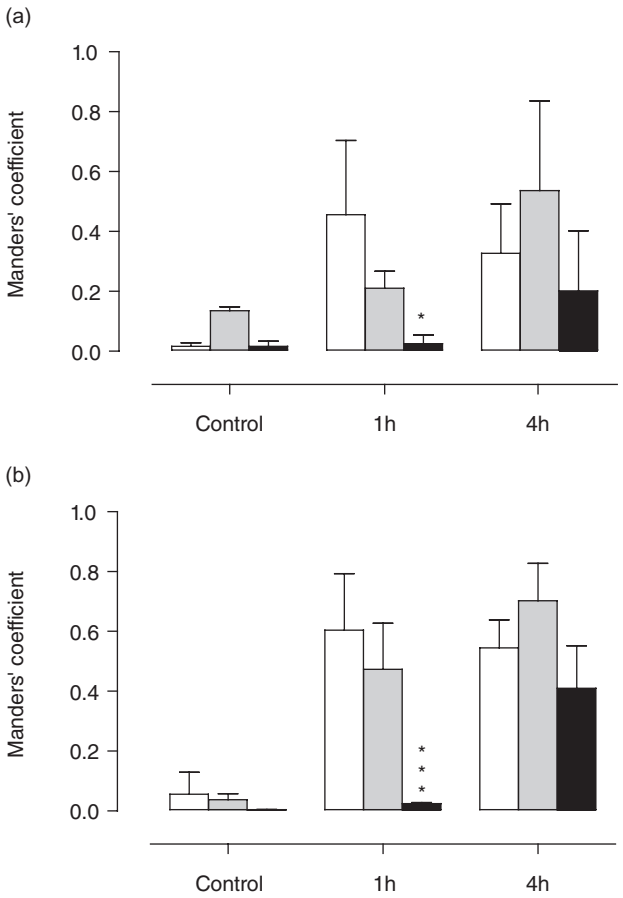

Figure 11. Co-localization analyses of DAF-FM (a) or APF (b) with Mitotracker Red in tobacco mesophyll cells at different times following treatment with the complex III inhibitor AA (10 μM). Tobacco lines tested include the WT (open bars), a transgenic line with suppressed levels of AOX (RI29, shaded bars) and a transgenic line overexpressing AOX (B7, black bars). In this analysis, the Manders' coefficient represents the fraction of pixels from the red fluorescence channel (mitochondria) that overlap with the green fluorescence channel [NO in (a) or $ONOO^-$ in (b)]. Data are the mean ± SE of three independent experiments. Data were analysed by two-way ANOVA followed by a Bonferroni post-test to compare at each time point the WT line with each transgenic line. Number of asterisks indicates the level of significant difference: $*P < 0.05$; $***P < 0.001$. Data points without an asterisk are not significantly different from the WT.

appear to be due to a constitutive up-regulation of scavenging mechanisms since we saw no change in control MnSOD activity in these plants relative to WT. It may be that some broader adjustment of the levels of ETC components during development allows the transgenic plants greater resilience (at least in terms of ROS and RNS generation) towards cytochrome pathway limitations. Regardless of the mechanism, however, it was clear that this increased resilience was able to only delay and not prevent the expected increase in mitochondrial O_2^- and NO.

The delay in O_2^- generation in RI29 in response to AA is reminiscent of the delay in the O_2^- burst seen after infection of RI9 and RI29 plants with pv. *maculicola*. In other words, both pv. *maculicola* infection and inhibition of complex III produced similar phenomenon. In WT plants, each of these treatments resulted in a rapid O_2^- burst, while in knockdown plants, each of these treatments resulted in a delayed burst. This hints that one consequence of the infection with pv. *maculicola* is a targeting of complex III function. At present, very little is known regarding the impact of bacterial infections on mitochondrial function. One aspect of pv. *maculicola* infection of WT tobacco plants that is less pronounced with pv. *phaseolicola* is the rapid accumulation of SA (Cvetkovska & Vanlerberghe 2012b). Interestingly, a few studies have shown that ETC function is impacted by SA, but the details of this impact are still poorly understood (Xie & Chen 1999; Norman *et al*. 2004; Battaglia, Salvi & Toninello 2005; van der Merwe & Dubery 2006). One such study, performed using isolated mitochondria from plant suspension cells, has suggested an impact of SA on the Q-cycle of complex III (de Souza *et al*. 2011). It has also been reported that complex III inhibitors with different sites of action display a differential ability to elicit cell death in tobacco cells (Robson, Zhao & Vanlerberghe 2008). More broadly, it is recognized that plant mitochondria are a target of *P. syringae* effector proteins (Greenberg & Vinatzer 2003; Block *et al*. 2010).

CONCLUSIONS

We previously showed that RI9 and RI29 plants lacking AOX display constitutive higher levels of mitochondrial O_2^- and NO, indicating that AOX is an important determinant of ROS and RNS generation by the respiratory chain (Cvetkovska & Vanlerberghe 2012a). Our results with AA are consistent with this hypothesis. In particular, while AA treatment of WT plants resulted in a transient burst of both O_2^- and NO, both bursts were prevented in plants that overexpress AOX. This shows that over-reduction of the respiratory chain by AA can increase single electron leak to O_2 or nitrite, but that this is prevented if sufficient AOX is present to maintain electron flow.

Our study provides a compelling example of a biological process, in this case, a response to bacterial pathogen, in which AOX appears to play a central role in defining a mitochondrial ROS signature. While tobacco plants do not normally display an O_2^- burst in response to pv. *phaseolicola*, RI9 and RI29 plants, unable to induce AOX, do display such a burst. However, we did not see changes in the dynamics of NO generation by these plants in response to bacteria. The transgenic plants did not show an NO burst in response to pv. *phaseolicola* and they did not show a delayed NO burst, like they did for O_2^-, in response to pv. *maculicola*. This suggests that, while AOX level is a key determinant of mitochondrial ROS dynamics in response to bacteria, it may not be a principal determinant of mitochondrial NO dynamics in response to bacteria.

ACKNOWLEDGMENTS

The authors thank Dr K. Yoshioka and Dr R. Harrison, each at the University of Toronto, for the different bacteria and advice on fluorescence imaging, respectively. We gratefully acknowledge the financial support of the Natural Sciences and Engineering Research Council of Canada.

REFERENCES

Amirsadeghi S., Robson C.A., McDonald A.E. & Vanlerberghe G.C. (2006) Changes in plant mitochondrial electron transport alter cellular levels of reactive oxygen species and susceptibility to cell death signaling molecules. *Plant and Cell Physiology* **47,** 1509–1519.

Amirsadeghi S., Robson C.A. & Vanlerberghe G.C. (2007) The role of the mitochondrion in plant responses to biotic stress. *Physiologia Plantarum* **129,** 253–266.

Battaglia V., Salvi M. & Toninello A. (2005) Oxidative stress is responsible for mitochondrial permeability transition induction by salicylate in liver mitochondria. *Journal of Biological Chemistry* **280,** 33864–33872.

Block A., Guo M., Li G., Elowsky C., Clemente T.E. & Alfano J.R. (2010) The *Pseudomonas syringae* type III effector HopG1 targets mitochondria, alters plant development and suppresses plant innate immunity. *Cellular Microbiology* **12,** 318–330.

Bolte S. & Cordelieres F.P. (2006) A guided tour into subcellular colocalization analysis in light microscopy. *Journal of Microscopy* **224,** 213–232.

Chaki M., Valderrama R., Fernández-Ocaña A.M., *et al*. (2009) Protein targets of tyrosine nitration in sunflower (*Helianthus annuus* L.) hypocotyls. *Journal of Experimental Botany* **60,** 4221–4234.

Chaki M., Valderrama R., Fernández-Ocaña A.M., *et al*. (2011) High temperature triggers the metabolism of S-nitrosothiols in sunflower mediating a process of nitrosative stress which provokes the inhibition of ferredoxin-NADP reductase by tyrosine nitration. *Plant, Cell & Environment* **34,** 1803–1818.

Cheng D.-D., Jia Y.-J., Gao H.-Y., Zhang L.-T., Zhang Z.-S., Xue Z.-C. & Meng Q.-W. (2011) Characterization of the programmed cell death induced by metabolic products of *Alternaria alternata* in tobacco BY-2 cells. *Physiologia Plantarum* **141,** 117–129.

Coll N.S., Epple P. & Dangl J.L. (2011) Programmed cell death in the plant immune response. *Cell Death and Differentiation* **18,** 1247–1256.

Cvetkovska M. & Vanlerberghe G.C. (2012a) Alternative oxidase modulates leaf mitochondrial concentrations of superoxide and nitric oxide. *New Phytologist* **195,** 32–39.

Cvetkovska M. & Vanlerberghe G.C. (2012b) Coordination of a mitochondrial superoxide burst during the hypersensitive response to bacterial pathogen in *Nicotiana tabacum*. *Plant, Cell & Environment* **35,** 1121–1136.

Finnegan P.M., Soole K.L. & Umbach A.L. (2004) Alternative mitochondrial electron transport proteins in plants. In *Plant Mitochondria: From Genome to Function* (eds D.A. Day, A.H. Millar & J. Whelan), pp. 163–230. Kluwer Academic Publishers, Dordrecht, The Netherlands.

Garmier M., Priault P., Vidal G., Driscoll S., Djebbar R., Boccara M., Mathieu C., Foyer C.H. & De Paepe R. (2007) Light and oxygen are not required for harpin-induced cell death. *Journal of Biological Chemistry* **282,** 37556–37566.

Gaupels F., Spiazzi-Vandelle E., Yang D. & Delledonne M. (2011) Detection of peroxynitrite accumulation in *Arabidopsis thaliana* during the hypersensitive defense response. *Nitric Oxide* **25,** 222–228.

Gilliland A., Singh D.P., Hayward J.M., Moore C.A., Murphy A.M., York C.J., Slator J. & Carr J.P. (2003) Genetic modification of alternative respiration has differential effects on antimycin A-induced versus salicylic acid-induced resistance to *Tobacco mosaic virus*. *Plant Physiology* **132,** 1518–1528.

Gleason C., Huang S., Thatcher L.F., Foley R.C., Anderson C.R., Carroll A.J., Millar A.H. & Singh K.B. (2011) Mitochondrial complex II has a key role in mitochondrial-derived reactive oxygen species influence on plant stress gene regulation and defense. *Proceedings of the National Academy of Science* **108,** 10768–10773.

Greenberg J.T. & Vinatzer B.A. (2003) Identifying type III effectors of plant pathogens and analyzing their interaction with plant cells. *Current Opinion in Microbiology* **6,** 20–28.

Gupta K.J., Igamberdiev A.U., Manjunatha G., Segu S., Moran J.F., Neelawarne B., Bauwe H. & Kaiser W.M. (2011) The emerging roles of nitric oxide (NO) in plant mitochondria. *Plant Science* **181,** 520–526.

Hamanaka R.B. & Chandel N.S. (2010) Mitochondrial reactive oxygen species regulate cellular signaling and dictate biological outcomes. *Trends in Biochemical Sciences* **35,** 505–513.

King E.O., Ward M.K. & Raney D.E. (1954) Two simple media for the demonstration of pyocyanin and fluorescein. *Journal of Laboratory and Clinical Medicine* **44,** 301–307.

Király L., Hafez M., Fodor J. & Király Z. (2008) Suppression of tobacco mosaic virus-induced hypersensitive-type necrotization in tobacco at high temperature is associated with downregulation of NADPH oxidase and superoxide and stimulation of dehydroascorbate reductase. *Journal of General Virology* **89,** 799–808.

Kojima H., Urano Y., Kikuchi K., Higuchi T., Hirata Y. & Nagano T. (1999) Fluorescent indicators for imaging nitric oxide production. *Angewandte Chemie International Edition* **38,** 3209–3212.

Lacomme C. & Roby D. (1999) Identification of early marker genes of the hypersensitive response in *Arabidopsis thaliana*. *FEBS Letters* **459,** 149–153.

Lee W.-S., Fu S.-F., Verchot-Lubicz J. & Carr J.P. (2011) Genetic modification of alternative respiration in *Nicotiana benthamiana* affects basal and salicylic acid-induced resistance to potato virus X. *BMC Plant Biology* **11,** 41.

Leitner M., Vandelle E., Gaupels F., Bellin D. & Delledonne M. (2009) NO signals in the haze. Nitric oxide signaling in plant defense. *Current Opinion in Plant Biology* **12,** 451–458.

van der Merwe J.A. & Dubery I.A. (2006) Benzothiazole inhibits mitochondrial NADH:ubiquinone oxidoreductase in tobacco. *Journal of Plant Physiology* **163,** 877–882.

Modolo L.V., Augusto O., Almeida I.M.G., Magalhaes J.R. & Salgado I. (2005) Nitrite as the major source of nitric oxide production by *Arabidopsis thaliana* in response to *Pseudomonas syringae*. *FEBS Letters* **579,** 3814–3820.

Møller I.M. (2001) Plant mitochondria and oxidative stress: electron transport, NADPH turnover, and metabolism of reactive oxygen species. *Annual Review of Plant Physiology and Plant Molecular Biology* **52,** 561–591.

Mur L.A.J., Kenton P., Lloyd A.J., Ougham H. & Prats E. (2008) The hypersensitive response; the centenary is upon us but how much do we know? *Journal of Experimental Botany* **59,** 501–520.

Murphy M.P. (2009) How mitochondria produce reactive oxygen species. *Biochemistry Journal* **417,** 1–13.

Naton B., Hahlbrock K. & Schmelzer E. (1996) Correlation of rapid cell death with metabolic changes in fungus-infected, cultured parsley cells. *Plant Physiology* **112,** 433–444.

Norman C., Howell K.A., Millar A.H., Whelan J.M. & Day D.A. (2004) Salicylic acid is an uncoupler and inhibitor of mitochondrial electron transport. *Plant Physiology* **134,** 492–501.

Ordog S.H., Higgins V.J. & Vanlerberghe G.C. (2002) Alternative oxidase is not a critical component of plant viral resistance but may play a role in the hypersensitive response. *Plant Physiology* **129,** 1858–1865.

Pattanayak G.K., Venkataramani S., Hortensteiner S., *et al*. (2012) Accelerated cell death 2 suppresses oxidative bursts and modulates cell death in Arabidopsis. *The Plant Journal* **69,** 589–600.

Planchet E., Gupta K.J., Sonoda M. & Kaiser W.M. (2005) Nitric oxide emission from tobacco leaves and cell suspensions: rate limiting factors and evidence for the involvement of mitochondrial electron transport. *The Plant Journal* **41,** 732–743.

Poyton R.O., Ball K.A. & Castello P.R. (2009) Mitochondrial generation of free radicals and hypoxic signaling. *Trends in Endocrinology and Metabolism* **20,** 332–340.

Robinson K.M., Janes M.S. & Beckman J.S. (2008) The selective detection of mitochondrial superoxide by live cell imaging. *Nature Protocols* **3,** 941–947.

Robson C.A., Zhao D.Y. & Vanlerberghe G.C. (2008) Interactions between mitochondrial electron transport, reactive oxygen species, and the susceptibility of *Nicotiana tabacum* cells to programmed cell death. *Botany* **86,** 278–290.

Serrano I., Romero-Puertas M.C., Rodríguez-Serrano M., Sandalio L.M. & Olmedilla A. (2012) Peroxynitrite mediates programmed cell death both in papillar cells and in self-incompatible pollen in the olive (*Olea europaea* L.). *Journal of Experimental Botany* **63,** 1479–1493.

Setsukinai K.-I., Urano Y., Kakinuma K., Majima H.J. & Nagano T. (2003) Development of novel fluorescence probes that can reliably detect reactive oxygen species and distinguish specific species. *Journal of Biological Chemistry* **278,** 3170–3175.

Simons B.H., Millenaar F.F., Mulder L., van Loon L.C. & Lambers H. (1999) Enhanced expression and activation of alternative oxidase during infection of Arabidopsis with *Pseudomonas syringae* pv tomato. *Plant Physiology* **120,** 529–538.

de Souza W.R., Vessecchi R., Dorta D.J., Uyemura S.A., Curti C. & Vargas-Rechia C.G. (2011) Characterization of *Rubus fruticosus* mitochondria and salicylic acid inhibition of reactive oxygen species generation at Complex III/Q cycle: potential implications for hypersensitive response of plants. *Journal of Bioenergetics and Biomembranes* **43,** 237–246.

Spoel S.H. & Loake G.J. (2011) Redox-based protein modifications: the missing link in plant immune signaling. *Current Opinion in Plant Biology* **14,** 358–364.

Torres M.A. (2010) ROS in biotic interactions. *Physiologia Plantarum* **138,** 414–429.

Torres M.A., Jones J.D.G. & Dangl J.L. (2006) Reactive oxygen species signaling in response to pathogens. *Plant Physiology* **141,** 373–378.

Vandelle E. & Delledonne M. (2011) Peroxynitrite formation and function in plants. *Plant Science* **181,** 534–539.

Vanlerberghe G.C. & McIntosh L. (1992) Coordinate regulation of cytochrome and alternative pathway respiration in tobacco. *Plant Physiology* **100,** 1846–1851.

Vanlerberghe G.C. & McIntosh L. (1994) Mitochondrial electron transport regulation of nuclear gene expression: studies with the alternative oxidase gene of tobacco. *Plant Physiology* **105,** 867–874.

Vellosillo T., Vicente J., Kulasekaran S., Hamberg M. & Castresana C. (2010) Emerging complexity in reactive oxygen species production and signaling during the response of plants to pathogens. *Plant Physiology* **154,** 444–448.

Vidal G., Ribas-Carbo M., Garmier M., Dubertret G., Rasmusson A.G., Mathieu C., Foyer C.H. & De Paepe R. (2007) Lack of respiratory chain complex I impairs alternative oxidase engagement and modulates redox signaling during elicitor-induced cell death in tobacco. *The Plant Cell* **19,** 640–655.

Wang J., Rajakulendran N., Amirsadeghi S. & Vanlerberghe G.C. (2011) Impact of mitochondrial alternative oxidase expression on the response of *Nicotiana tabacum* to cold temperature. *Physiologia Plantarum* **142,** 339–351.

Xie Z. & Chen Z. (1999) Salicylic acid induces rapid inhibition of mitochondrial electron transport and oxidative phosphorylation in tobacco cells. *Plant Physiology* **120,** 217–225.

Yao N. & Greenberg J.T. (2006) *Arabidopsis* accelerated cell death2 modulates programmed cell death. *The Plant Cell* **18,** 397–411.

Yao N., Tada Y., Sakamoto M., Nakayashiki H., Park P., Tosa Y. & Mayama S. (2002) Mitochondrial oxidative burst involved in apoptotic response in oats. *The Plant Journal* **30,** 567–579.

Received 24 July 2012; received in revised form 4 September 2012; accepted for publication 8 September 2012

SUPPORTING INFORMATION

Additional Supporting Information may be found in the online version of this article:

Figure S1. Typical laser-scanning confocal microscope image of a tobacco mesophyll cell labeled for mitochondrial O_2^- with MitoSOX Red. The first panel from left shows the bright-field image, along with air spaces (as). The second panel shows the chlorophyll autofluorescence in blue (false coloration). In the third panel, mitochondrial O_2^- and the nucleus (marked with an arrow) are shown in red. The last panel is a merged image of all three previous panels. All images are maximum intensity projections of Z-series (8–16 μm in depth). Scale bar = 20 μm.

Figure S2. MnSOD (a), CuZnSOD (b) and FeSOD (c) activity in tobacco leaf at different times post-inoculation with *P. syringae* pv. *phaseolicola*. Tobacco lines tested included the WT (closed circle) and two transgenic lines with suppressed levels of AOX (RI9, open triangle; RI29, open square). Data are the mean ± SE of two independent experiments. Data are relative to the SOD activity of the WT at time 0, which was set to 1.

Figure S3. Laser-scanning confocal microscope images of cellular NO in tobacco mesophyll cells at different times post-inoculation with *P. syringae* pv. *phaseolicola*. Tobacco lines tested include the WT and two transgenic lines with suppressed levels of AOX (RI9, RI29). All images are maximum intensity projections of Z-series (8–16 μm in depth) and are representative results from three independent experiments, each of which showed similar results. All images are double-labeled with DAF-FM and Mitotracker Red to image both NO (green) and mitochondria (red). Co-localization of these signals is yellow. The control plants (mock-inoculated with H_2O) were similar at 4 h and 24 h, so only images taken at 24 h are shown here. Scale bar = 20 μm.

Figure S4. Laser-scanning confocal microscope images of cellular $ONOO^-$ in tobacco mesophyll cells at different times post-inoculation with *P. syringae* pv. *phaseolicola*. Tobacco lines tested include the WT and two transgenic lines with suppressed levels of AOX (RI9, RI29). All images are maximum intensity projections of Z-series (8–16 μm in depth) and are representative results from three independent experiments, each of which showed similar results. All images are double-labeled with APF and Mitotracker Red to image both $ONOO^-$ (green) and mitochondria (red). Co-localization of these signals is yellow. The control plants (mock-inoculated with H_2O) were similar at 4 h and 24 h, so only images taken at 24 h are shown here. Scale bar = 20 μm.